Channelling Effects in Electron Induced X-Ray Emission from Diatomic Crystals

J. Taftø

Department of Physics, University of Oslo, Oslo, Norway

Z. Naturforsch. **34a**, 452–458 (1979); received February 10, 1979

The variation of x-ray emission with direction of the incident beam has been studied in diatomic crystals of ZnS, ZnSe and FeS_2 using an electron microscope at 80 keV attached with a Si(Li) x-ray detector. The interpretation is based on the Bloch wave picture taking into account absorption and diffuse scattering of the electrons.

Introduction

The variation of current density distribution over the unit cell with direction of the incident beam gives rise to anomalous absorption and other orientation effects in electron diffraction. One of these, the electron induced x-ray emission, was demonstrated to depend on the diffraction condition already in 1962 by Duncumb [1] and a theoretical treatment based on the Bloch wave considerations was given by Hirsch, Howie and Whelan [2].

The possibility of obtaining crystallographic information from this effect was discussed by Gjønnes and Høier [3] who showed theoretically that the orientation dependence could, at least in principle, be used for determination of e.g. solute atoms within the unit cell.

Relatively few experiments on x-ray emission under anomalous absorption or channelling conditions have been reported, however, despite the widespread use of x-ray spectrometers as auxiliary equipment to electron microscopes [4–8]. Compared to the similar effect in ion beam channelling which has already been utilized in solid state studies (e.g. Kool et al. [9]), electrons suffer from two disadvantages: The quite strong Bremsstrahlung which gives an appreciable background, and the strong diffuse scattering which tends to smear out the effect. On the other hand, the versatility of the electron beam instruments, e.g. the possibility of focussing the beams onto a very small area, simultaneous observations of diffraction patterns and images etc., and also the fact that the same effect can be observed from the energy loss of the electrons, may suggest a more detailed study of the channelling effects in x-ray emission, particularly for crystals containing more than one type of atoms.

In this paper some experiments showing orientation effects in x-ray emission from ZnS, ZnSe and FeS_2 are reported. The interpretation is based on the Bloch wave description. Qualitative two beam considerations as well as many beam calculations including absorption and diffuse scattering have been performed.

Experiment

The specimens were examined in a transmission electron microscope with an EDAX-spectrometer, operating at 80 kV. The electron beam divergence was of the order 1% of the Bragg angle for the shortest reciprocal lattice vectors (0.5 $Å^{-1}$) and the diameter of the beam on the specimen about 1 μm. The x-ray detector, a Si(Li)-crystal, had a collecting angle of about 10^{-4} sterads and was separated from the microscope vacuum system by a beryllium window.

Relatively flat areas at the edges of ion thinned specimens were analyzed. The approximate thickness was determined from the thickness fringes, and the direction of the incident beam from the Kikuchi patterns (Figure 1).

The experiments were done in directions where the two types of atoms are projected into different positions. Figures 2a, b and c show the ratio between the intensity of the two K_α-lines in thin crystals ($\sim$ 1000 Å) of ZnS, ZnSe and FeS_2 in planar cases. Figure 2d shows the result from a considerably thicker FeS_2 crystal ($\sim$ 5000 Å) where the Bragg reflections were invisible.

Measurements near a zone axis, the (100)-projection of ZnS, are shown in Figure 3. To the right in the figure, i.e. at the end of the experiment, the K_α-ratio variation with direction is smeared out,

Reprint requests to J. Taftø. Fritz-Haber-Institut Abt. Prof. Molière, Faradayweg 4–6, D-1000 Berlin 33. Please order a reprint rather than making your own copy.

0340-4811 / 79 / 0400-0452 $ 01.00/0

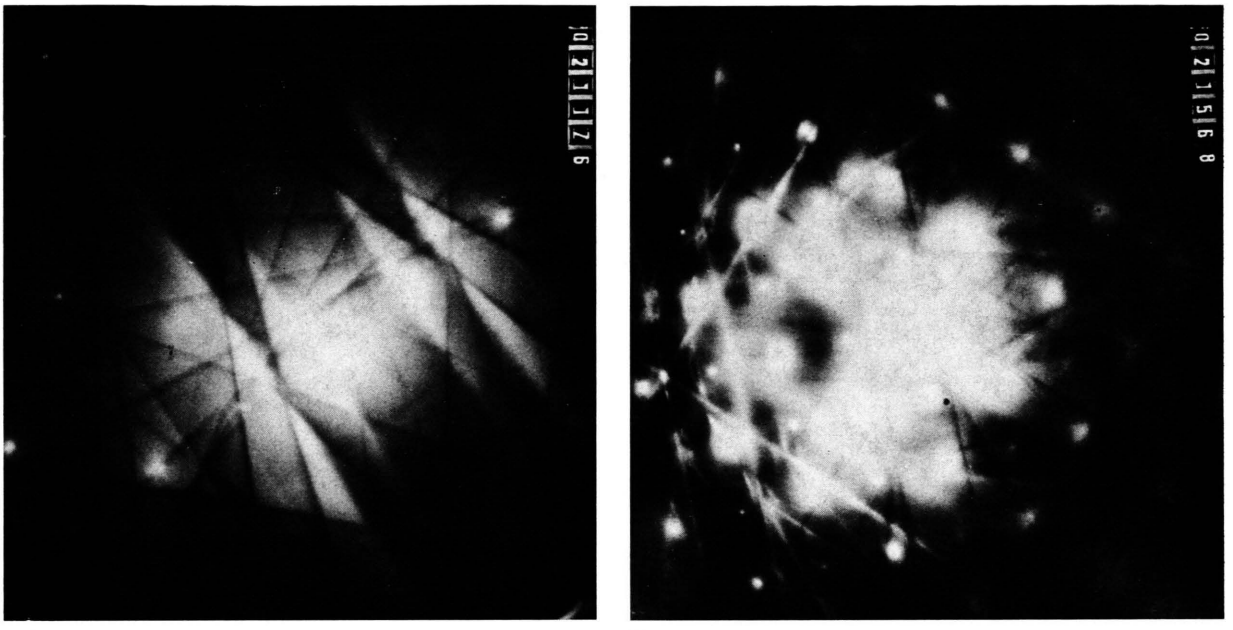

a) b)

Fig. 1. Examples showing the diffraction conditions under the x-ray measurements. a) (200)-plane of ZnS. b) (001)-projection of ZnS.

probably caused by radiation damage or contamination which were clearly seen in the Kikuchi patterns.

Theory

Anomalous absorption and direction dependent x-ray emission are caused by the nonuniform distribution of the incident electrons over the projected unit cell combined with the localization of the potential fluctuations and the x-ray production sources.

Let $B(\boldsymbol{r})$ be the probability that an electron at the coordinate $\boldsymbol{r}$ in the projected unit cell will produce secondary emission. Then the production in a crystal of thickness Z is:

$$\int_0^Z \int_{\substack{\text{unit}\\ \text{cell}}} B(\boldsymbol{r})\, I(\boldsymbol{r}, z)\, \mathrm{d}\boldsymbol{r}\, \mathrm{d}z \tag{1}$$

where $I(\boldsymbol{r}, z)$ is the current density distribution at a distance z from the entrance surface. For K-shell emission from medium or heavy atoms $B(\boldsymbol{r})$ can usually be looked upon as a δ-function at the mean atomic position because the current density varies slowly compared to the amplitude of the thermal vibrations and the width of the 1s distribution. Hence the problem is reduced to calculation of the current density at the position of the emitting atom:

$$\int_0^Z I(\boldsymbol{r}, z)\, \mathrm{d}z\,. \tag{2}$$

From the suggestion of Hall [4] the electrons which have undergone diffuse scattering are uniformly distributed over the unit cell. The electrons can then be divided into two categories as to whether they have been diffusely scattered or not. Following the treatment of Cherns et al. [7] and assuming the incident beam to be parallel the current density contribution from the electrons which have not undergone diffuse scattering can be written in terms of Bloch waves, $b^j(\boldsymbol{r})$:

$$I_{\mathrm{el}}(\boldsymbol{r}, z) = \sum_j \sum_{j'} C_0^j\, C_0^{j'*}\, b^j(\boldsymbol{r})\, b^{j'*}(\boldsymbol{r}) \cdot \exp[i(\gamma^j - \gamma^{j'})\, z] \exp[(-\mu^j - \mu^{j'})\, z]\,, \tag{3}$$

where γ^j are the anpassungen and $C_0{}^j$ Bloch wave coefficients. In the absorption parameters μ^j, the plasmon contribution should be excluded because the plasmon scattered electrons are strongly peaked in the forward direction and will behave approximately like the incident beam in producing x-rays unless the current density distribution changes

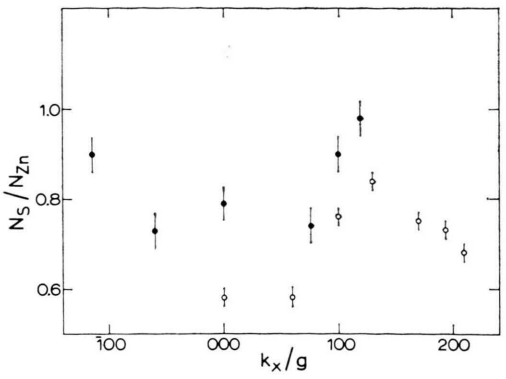

a)

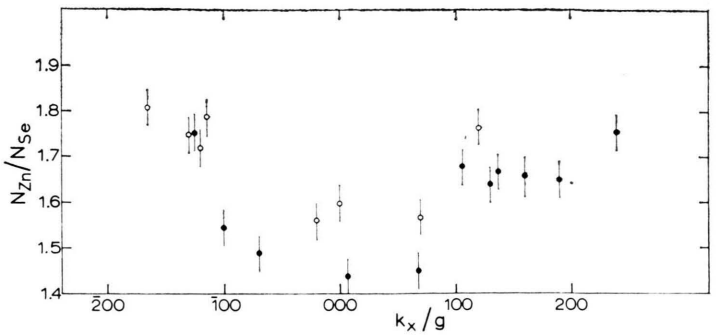

b)

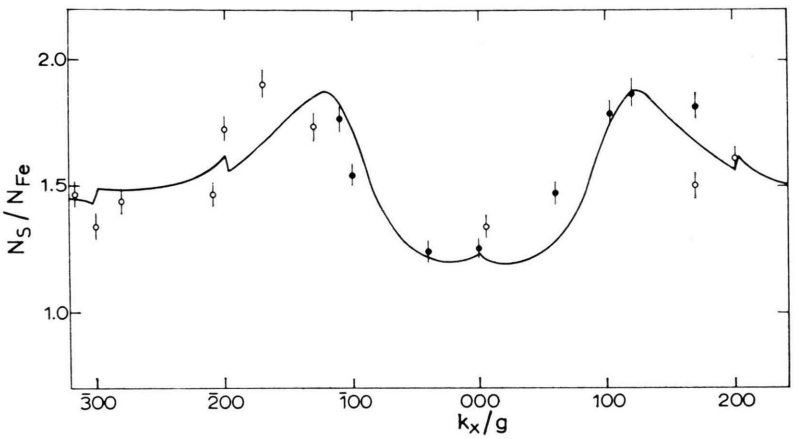

c)

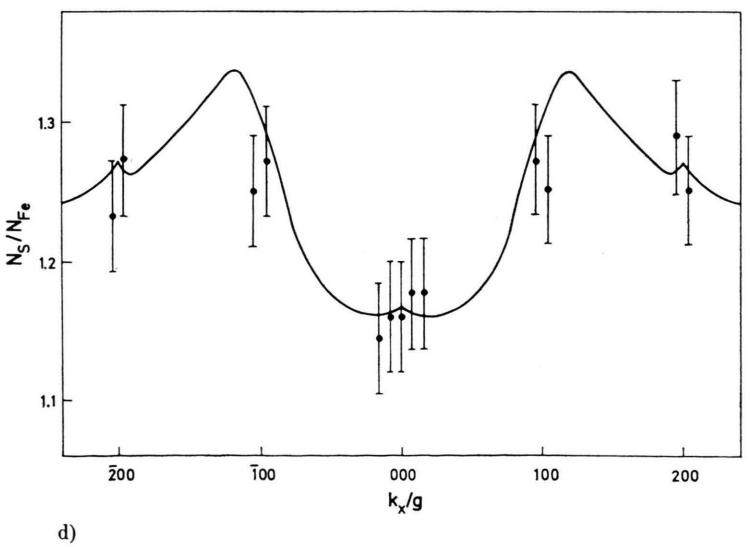

d)

Fig. 2. Ratio between the K_α-emission in planar cases.

a) ZnS. The thickness was about 1000 Å (open circles) and 3000 Å (full circles).
b) ZnSe. The open and filled circles represent different areas and probably different thicknesses.
c) Thin FeS_2 crystal.
d) Thick FeS_2 crystal. There is no significant difference with respect to diffraction conditions for the groups of measurements positioned close together. The separation within each group is introduced for display purpose only.

The curves in c) and d) show 7 beam calculations [Eq. (5)] for 1500 Å and 5000 Å thickness respectively. The imaginary Fourier potential was chosen to be 0.09 times the real ($U_g' = 0.09\ U_g$) and the normal absorption parameter $\mu_0 = 0.0019$ Å^{-1}.

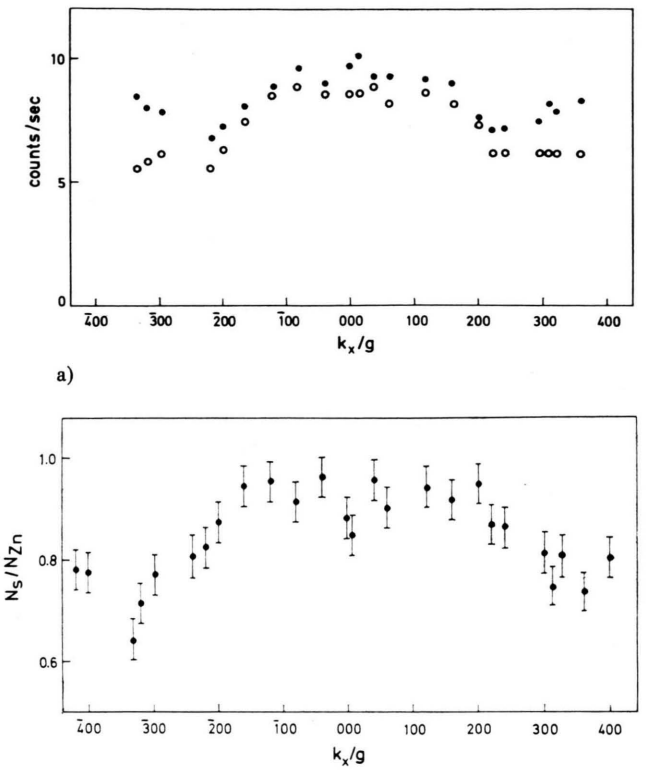

Fig. 3. K_α-emission in the (001)-projection for ZnS. a) Count rate for Zn (filled circles) and S (open circles). b) The ratio between the counts from S and Zn.

rapidly with direction compared to the angular spread of the Bragg peaks caused by the plasmon scattering.

The remaining electrons have undergone diffuse scattering, and from the assumption above they are uniformly distributed over the unit cell, so that the intensity contribution from them is

$$I_d(\boldsymbol{r}, z) = 1 - \sum_j |C_0^j|^2 \exp(-2\mu^j z) . \quad (4)$$

The variation of x-ray production with direction for an atom at the coordinate $\boldsymbol{r}$ in the unit cell is now found by integration over the thickness:

$$\begin{aligned} &\int_0^Z (I_{el}(\boldsymbol{r}, z) + I_d(\boldsymbol{r}, z))\, dz \\ &= Z + \sum_j \frac{1}{2\mu^j} |C_0^j|^2 (\exp(-2\mu^j Z) - 1) \\ &\quad + \sum_j \sum_{j'} \sum_h \sum_{h'} \frac{1}{(-\mu^j - \mu^{j'}) + i(\gamma^j - \gamma^{j'})} \\ &\quad \cdot C_0^j C_0^{j'*} C_h^j C_h^{j'*} \exp[i\boldsymbol{r}(\boldsymbol{h} - \boldsymbol{h}')] \quad (5) \\ &\quad \cdot \{\exp[(-\mu^j - \mu^{j'}) Z + i(\gamma^j - \gamma^{j'}) Z] - 1\} . \end{aligned}$$

Let us now look at the x-ray production from a multiple diffuse scattering point of view. A theory for multiple diffuse scattering has been given by Høier [10] and applied to calculation of Kikuchi band contrast. But calculation of the background contribution to $I(\boldsymbol{r}, z)$ is complicated especially in the x-ray production case where the whole pattern of diffuse and multiple scattering should be considered. Neglecting the interference between the different Bloch waves, we may write the current density:

$$I(\boldsymbol{r}, z) = \sum_j \int_{\boldsymbol{s}} A^j(\boldsymbol{s}, z) \, |b^j(\boldsymbol{r}, \boldsymbol{s})|^2 \, d\boldsymbol{s} , \quad (6)$$

where the weight factors A^j for the Bloch wave states are governed by diffuse scattering in and out of these states [11]:

$$\begin{aligned} \frac{dA^j(\boldsymbol{s})}{dz} &= -\mu^j(\boldsymbol{s}) A^j(\boldsymbol{s}) \\ &\quad + \int_{\boldsymbol{s}'} \sum_{j'} A^{j'}(\boldsymbol{s}') P^{jj'}(\boldsymbol{s}, \boldsymbol{s}') \, d\boldsymbol{s}' , \quad (7) \end{aligned}$$

where $\boldsymbol{s}$ are scattering vectors inside the first Brillouin zone and $P^{jj'}(\boldsymbol{s}, \boldsymbol{s}')$ the probability for diffuse scattering between the states j', $\boldsymbol{s}'$ and j, $\boldsymbol{s}$. Note that

$$\int_{\boldsymbol{s}'} \sum_{j'} P^{jj'}(\boldsymbol{s}, \boldsymbol{s}') = \mu^j(\boldsymbol{s}) .$$

Numerical solution of these equations is hardly feasible, because of the large number of coefficients involved and because the $P^{jj'}(\boldsymbol{s}, \boldsymbol{s}')$ are not known.

Nevertheless some simple, tentative conclusions can be drawn. In the central part of the pattern where A^j are large, absorption will drain intensity away from Bloch waves with high μ^j, leaving the low absorption Bloch waves which contribute to the channelling pattern. Further out in the pattern A^j will be governed mainly by scattering into the Bloch waves, and preferentially into those with high absorption, i.e. of blocking type, according to the reciprocity theorem which can be written $P^{jj'}(\boldsymbol{s}, \boldsymbol{s}') = P^{j'j}(\boldsymbol{s}', \boldsymbol{s})$. It seems to follow from this argument that the total contribution from the diffuse scattering may be reasonably well represented by a uniform distribution over the unit cell in accordance with the suggestion of Hall [4].

Although many beam calculations including absorption and interference between the Bloch waves are necessary for a quantitative treatment, much insight can be gained from simpler considerations. If interference and absorption are neglected

the current density can be written:

$$I(\boldsymbol{r}) = \sum_j |C_0{}^j|^2 \, |b^j(\boldsymbol{r})|^2 . \tag{8}$$

Interpretations and Discussions

In the planar case experiments, for which the atomic arrangements are shown in Fig. 4, there is a rapid change of K_α-ratio on going through the Bragg position for the first order reflections. This can be explained qualitatively from two beam considerations neglecting absorption and interference between the Bloch waves (Eq. (8)), the effect of which is mainly to smear out the variation with direction.

The symmetrical Bloch wave will have density maximum at the origin in real space whereas the antisymmetrical have minimum at that position. On choosing the origin so that the Fourier potential is positive, the symmetrical Bloch wave is strongly excited inside the reflecting position (negative excitation error) and the antisymmetrical outside. For the cases studied here the Fourier potential for the first order reflections are positive when origin is at the heaviest atom involved. Hence the ratio between the current density at the lightest and the heaviest atom I_L/I_H and consequently the ratio between the K_α-emission, N_L/N_H will increase on changing the excitation error from negative to positive (Figure 5). Although not observed due to insufficient experimental data, a similar change in ratio is expected near the Bragg position for the second order reflection in FeS_2, but not for ZnS and ZnSe where the symmetrical Bloch wave will hit both types of atoms and the antisymmetrical will avoid both. These considerations agree with six beam calculations for ZnS (Fig. 6) where we notice that rapid changes in I_s/I_{zn} occur at reflections to which the two types atoms scatter out of phase.

The results of the two beam and the six beam calculations were not much different in the neighbourhood of the Bragg positions i.e. diffraction conditions where the variation of x-ray emission is most easily seen. Therefore two beam treatments, which can be solved analytically, were found sufficient also when absorption and interference between the Bloch waves are taken into account (Eq. (5)). Calculations were done for directions where the ratio I_L/I_H is about maximum and minimum, respectively. In order to discuss the thickness dependence two situations were treated:

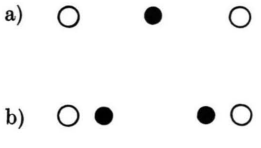

Fig. 4. Atomic arrangements along the (200)-direction. a) ZnS (Zn no space Se). b) FeS_2. Open circle Fe, filled circle space S.

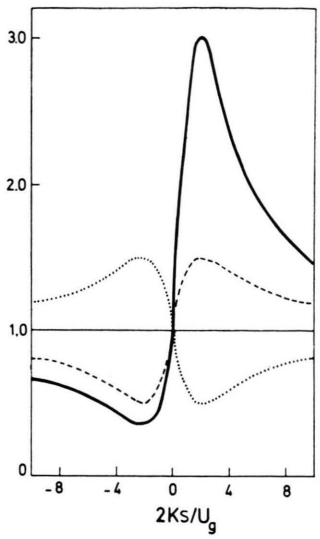

Fig. 5. Two beam calculations [Eq. (8)] of the ratio between the current density in the middle of the channel and at the origin (full line). Dotted lines show the current density at the two types of positions.

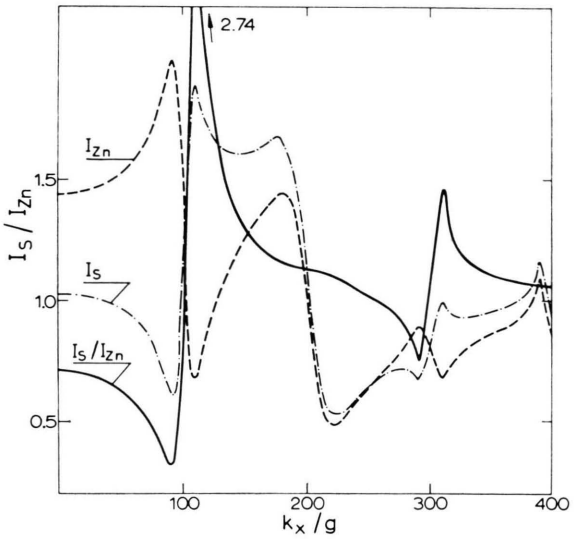

Fig. 6. 6 beam calculations [Eq. (8)] of the current density at the Zn and S atoms in ZnS.

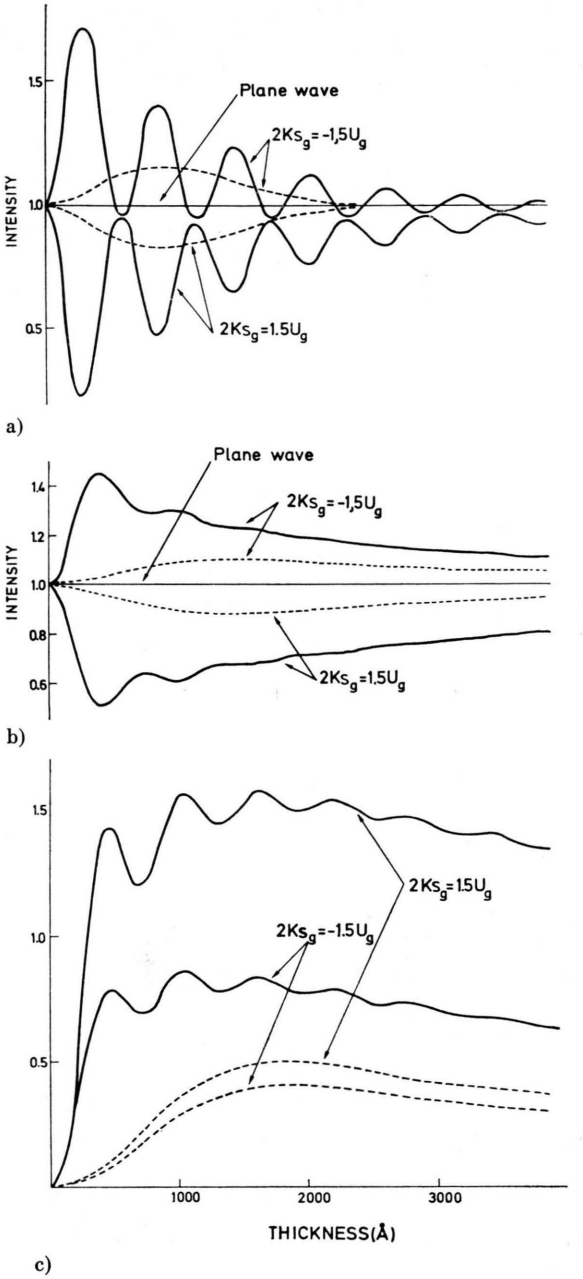

Fig. 7. Comparison, based on two beam calculations, between Si and ZnS at 80 keV. Full line: The intensity at the atomic position in Si for $g = (220)$. Dotted line: The intensity at the Zn atoms in ZnS when $g = (200)$. a) Intensity variations with thickness. b) Integrated intensity [Equation (5)]. c) Signal/noise ratio variation with thickness. The ratio is defined as

$$\frac{|Z - \int_0^Z I(z)\,dz|}{\sqrt{\int_0^Z I(z)\,dz}}.$$

1. Relatively short extinction length and low normal absorption.
2. Considerably larger extinction length and higher normal absorption.

For the first case the (220)-reflection in silicon was chosen. Here the normal and the anomalous absorption are well known. For the second case the (200)-reflection in ZnS was selected. The extinction length was taken from six beam calculations and was found to be six times that for the (220)-reflection in Si. The normal absorption was assumed to be twice that of Si.

In Fig. 7 the results of the calculations are presented. Only the current density at the Zn and Si atoms are shown. At the S atoms and in the middle of the channel for Si the current density is complementary. The observed variation of N_S/N_{Zn} is about 1.4 for 1000 Å as well as for 3000 Å whereas we get 1.5 and 1.3 from the calculations indicating the choise of absorption parameters to be reasonable. Due to shorter extinction length and lower absorption the effect is more pronounced in Si. From calculations of the similar ratio, i.e. the ratio between the current density in the middle of the channel and at the Si atoms changes with a factor 3.2 at 1500 Å which is the optimum thickness for detecting the effect according to signal/noise ratio calculations (Figure 7 c).

The observed direction dependence is less in ZnSe than in ZnS, probably due to higher normal

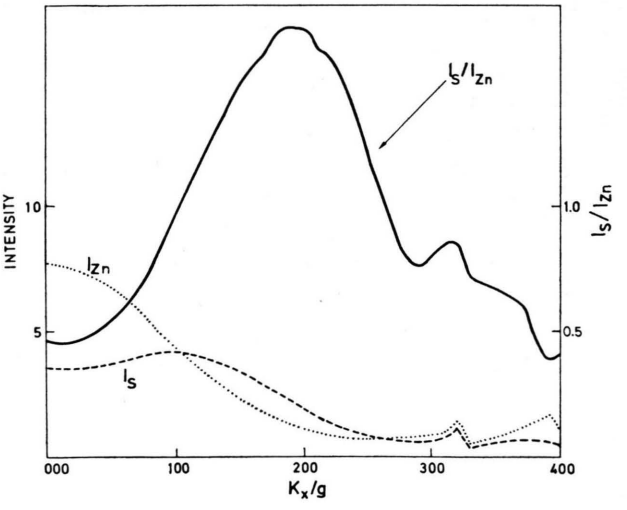

Fig. 8. 26 beam calculation of variations of the current density in the (001)-projection of ZnS.

absorption and the even larger extinction length for the (200)-reflection.

Although the S-atoms are not in the middle of the channel in FeS_2 the effect is more clearly seen than in ZnS. The reason for this may be the shorter extinction length and the better conservation of the antisymmetrical Bloch wave with thickness which agrees with the fact that the effect was observed for quite thick crystals of FeS_2 (Figure 2d). Seven beam calculations including anomalous absorption and diffuse scattering (Eq. (5)) show good agreement with the experimental results (Figure 2c, d).

Also in the (001)-projection of ZnS the observations (Fig. 3) can be explained qualitatively from simplified calculations excluding thickness dependence and absorption (Equation (8)). Calculations with 26 beams are shown in Figure 8.

Conclusions

The variation of electron induced x-ray emission with direction of the incident beam has been studied for diatomic crystals which are well suited for that purpose because the normalization problem can be avoided by observing the ratio between the x-ray emission from the two types af atoms.

When only one strong reflection is close to the Bragg position, the effect can be explained qualitatively from two beam considerations neglecting absorption and interference between the Bloch waves. The observed effect is, however, much smaller, mainly due to diffuse scattering. Application of the reciprocity theorem indicates that the electrons which have undergone diffuse scattering behave approximately like plane waves on the average, in accordance with the suggestion of Hall [4]. Calculations based on this approximation and taking into account the interference between the Bloch waves as pointed out by Cherns et al. [7], show fairly good agreement with the experimental results.

Calculations for two different cases show that the possibilities of observing the effect depend strongly upon the extinction lengths and the absorption parameters. With decreasing absorption parameters and extinction lengths the effect is more easily detected. Estimates of signal/noise ratio indicate that the variations with direction are as large in silicon crystals containing about 3% foreign atoms in the channels as being the case for ZnS. The effect is most easily seen at strong reflections where the extinction lengths are shortest and where also the washing out effect caused by divergence of the incident beam and plasmon scattering is less enhanced.

The method may be useful for determination of atomic positions in favourable cases, particularly in small crystals where conventional crystallographic methods are difficult to utilize, but the efficiency of the present instruments, which detect only a tiny fraction of the produced x-rays, seems to be too small.

Acknowledgement

The author is grateful to Dr. J. Gjønnes for many helpful discussions.

[1] P. Duncumb, Phil Mag. **7**, 2101 (1962).
[2] P. B. Hirsch, A. Howie, and M. J. Whelan, Phil. Mag. **7**, 2095 (1962).
[3] J. Gjønnes and R. Høier, Acta Cryst. **A 27**, 166 (1971).
[4] C. R. Hall, Proc. Roy. Soc. London **A 295**, 140 (1966).
[5] R. Castaing, J. Henoc, and P. Henoc, C.R. Acad. Sci. Paris **B 264**, 803 (1967).
[6] T. Bronder and J. Jakschik, Rad. Effects **13**, 209 (1972).
[7] D. Cherns, A. Howie, and M. H. Jacobs, Z. Naturforsch. **28a**, 565 (1973).
[8] W. Ludwig and N. Niedrig, Phys. Lett. **61 A**, 201 (1977).
[9] W. H. Kool, L. W. Wiggers, F. P. Viehböck, and F. W. Saris, Rad. Effects **27**, 43 (1975).
[10] R. Høier, Acta Cryst. **A 29**, 663 (1973).
[11] J. Gjønnes and J. Taftø, Nuclear Inst. Methods **132**, 141 (1976).